Acta Mech Sinica (2006) 22: 40–45
DOI 10.1007/s10409-005-0090-2

RESEARCH PAPER

Zibing Zhang · Jing Lu · Qisheng Chen
V. Prasad

Thermoelastic stresses in SiC single crystals grown by the physical vapor transport method

Received: 18 April 2005 / Accepted: 1 August 2005 / Revised: 11 August 2005 / Published online: 20 January 2006

Abstract A finite element-based thermoelastic anisotropic stress model for hexagonal silicon carbide polytype is developed for the calculation of thermal stresses in SiC crystals grown by the physical vapor transport method. The composite structure of the growing SiC crystal and graphite lid is considered in the model. The thermal expansion match between the crucible lid and SiC crystal is studied for the first time. The influence of thermal stress on the dislocation density and crystal quality is discussed.

Keywords Silicon carbide · Physical vapor transport · Thermal stress · Thermoelastic · Thermal expansion match

1 Introduction

The growth of silicon carbide bulk crystals has made a significant progress in recent years. SiC wafers of 2 inches and 3 inches in diameter are now available for the fabrication of electronic and optoelectronic devices operating in high power, high temperature, high frequency and intense radiation conditions. Physical vapor transport (PVT) method is the most commonly-used technique for the growth of bulk SiC single crystals [1]. The process modeling of PVT growth is a powerful tool for the optimization of growth process and has attracted great research interests in recent years. Hofmann et al. [2] modeled the temperature distribution in a SiC growth system in which the growth temperature is 2573 K and the system pressure is up to 3500 Pa. Pons et al. [3] proposed a numerical scheme for the calculation of electromagnetic field originated by the induction heating. Chen et al. [4] for the first time proposed a growth kinetics model which assumes that the growth rate is proportional to the supersaturation of the SiC vapor species at the growth interface and the growth rates in a 75 mm growth system were predicted. Thermally induced stresses in the growing crystals were calculated in past years [5–9]. The dependence of thermal stress on growth conditions and the influence of thermal stress on dislocation formation were studied. However, in all the above models, only the SiC crystal was considered in the calculation of thermal stresses, and the thermal expansion match between SiC single crystal and graphite crucible lid was not studied. Since physical properties such as elastic constants and thermal expansion coefficient of SiC differ from those of graphite, the crucible lid should be considered in the calculation of thermal stresses in SiC crystals.

In this paper, thermally induced stresses in the growing SiC crystals in a 2-inch growth system are calculated by using a finite element-based thermoelastic anisotropic model. The composite structure of the SiC crystal and crucible lid is considered in the calculation of thermal stresses.

The project supported by the National Natural Science Foundation of China (10472126) and the Knowledge Innovation Program of Chinese Academy of Sciences
The English text was polished by Keren Wang

Z.B. Zhang · J. Lu · Q.S. Chen (✉)
Institute of Mechanics, Chinese Academy of Sciences,
Beijing 100080, China
E-mail: qschen@imech.ac.cn
Tel.: 86-10-62564199
Fax: 86-10-62615524

V. Prasad
Department of Mechanical and Materials Engineering,
Florida International University,
10555 W Flagler St., Miami,
FL 33174, USA

2 Physical and mathematical model

In the growth of SiC crystals by the physical vapor transport method, SiC charge powder is usually put in a graphite crucible where a high temperature in the range of 1800 °C-2600 °C is achieved by induction heating. A typical schematic of the growth chamber in the physical vapor transport growth of SiC crystals is shown in Fig. 1. When argon pressure is lowered from the atmospheric pressure to a certain growth pressure, the SiC charge at a higher temperature sublimates, the vapor species then goes upward and deposits on the seed

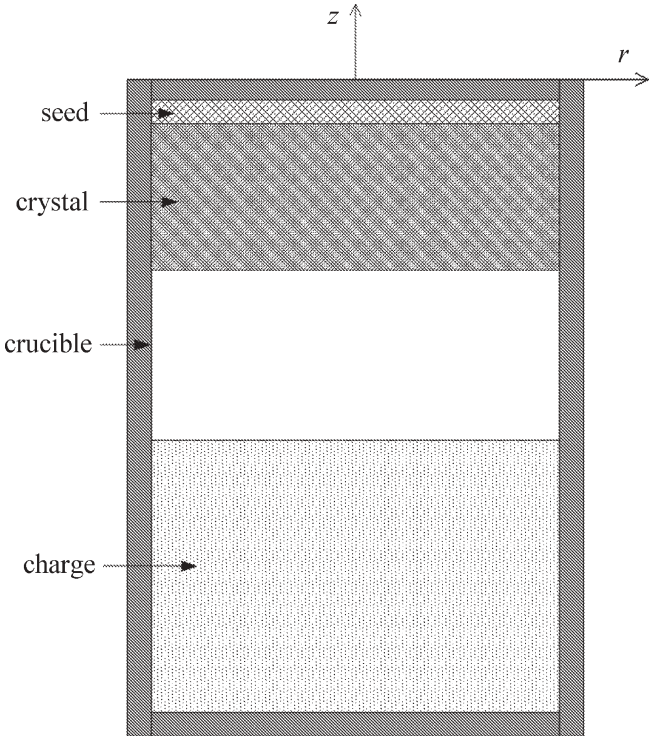

Fig. 1 Schematic of the growth chamber in the PVT growth of SiC crystals

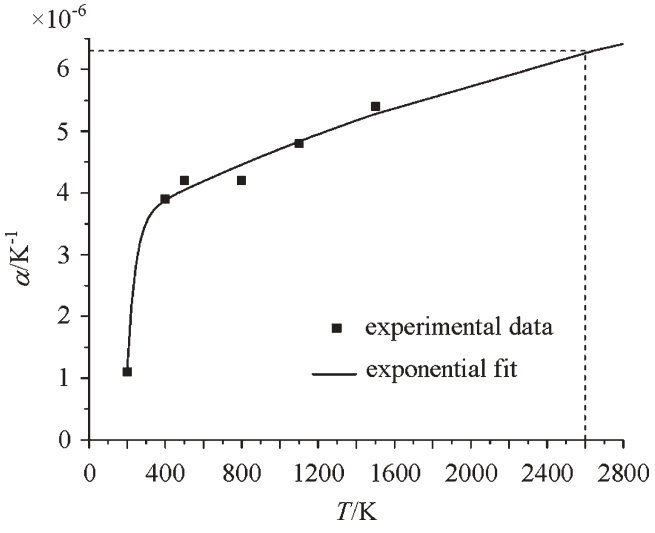

Fig. 2 Curve fitting of the thermal expansion coefficient-temperature relation for SiC crystal

with a lower temperature to form a SiC crystal. Due to non-uniformity of temperature distribution in the SiC crystal, thermal stresses are induced, which can cause plastic deformation and generation of dislocation during the growth process. Therefore it is very important to calculate the thermal stress distribution in the SiC bulk crystal in order to understand the mechanism of defect formation such as cracks, micropipes, dislocations and residual stresses. Since geometry and temperature distribution are axisymmetric, and 4H/6H-SiC is isotropic in the basal (0 0 0 1) plane, the thermal stress distribution can be considered as axisymmetric. By setting the z-axis of the coordinate system parallel to the crystallographic c-axis with $z = 0$ at the top of crucible lid (see Fig. 1), only the normal stress components σ_{rr}, $\sigma_{\phi\phi}$, σ_{zz} and shear stress component τ_{rz} need to be considered with $\tau_{r\phi} = \tau_{z\phi} = 0$. For the calculation of thermal stresses, the following equilibrium equations are used for the composite structure of SiC crystal and crucible lid:

$$\frac{1}{r}\frac{\partial}{\partial r}(r\sigma_{rr}) + \frac{\partial \tau_{rz}}{\partial z} - \frac{\sigma_{\phi\phi}}{r} = 0, \tag{1}$$

$$\frac{1}{r}\frac{\partial}{\partial r}(r\tau_{rz}) + \frac{\partial \sigma_{zz}}{\partial z} = 0. \tag{2}$$

The constitutive relation for a thermoelastic anisotropic body is taken as [10]

$$\begin{Bmatrix} \sigma_{rr} \\ \sigma_{\phi\phi} \\ \sigma_{zz} \\ \tau_{rz} \end{Bmatrix} = \begin{bmatrix} c_{11} & c_{12} & c_{13} & 0 \\ c_{12} & c_{22} & c_{23} & 0 \\ c_{13} & c_{23} & c_{33} & 0 \\ 0 & 0 & 0 & c_{44} \end{bmatrix} \times \begin{Bmatrix} \varepsilon_{rr} - \alpha_r(T - T_{\text{ref}}) \\ \varepsilon_{\phi\phi} - \alpha_\phi(T - T_{\text{ref}}) \\ \varepsilon_{zz} - \alpha_z(T - T_{\text{ref}}) \\ \gamma_{rz} \end{Bmatrix}. \tag{3}$$

In the above equation, ε_{rr}, $\varepsilon_{\phi\phi}$, ε_{zz}, and γ_{rz} are the strain components. c_{ij} the elastic constants. α_r, α_ϕ, α_z the thermal expansion coefficients in the r, ϕ and z directions, respectively; and T_{ref} is the reference temperature. The strains are defined as

$$\begin{aligned} \varepsilon_{rr} &= \frac{\partial u}{\partial r}, \\ \varepsilon_{\phi\phi} &= \frac{u}{r}, \\ \varepsilon_{zz} &= \frac{\partial w}{\partial z}, \\ \varepsilon_{rz} &= \frac{\partial u}{\partial z} + \frac{\partial w}{\partial r}, \end{aligned} \tag{4}$$

where u and w are the displacements in the radial and axial directions, respectively.

On the top of the crucible lid, it is assumed that the lid is bound to the graphite susceptor. The corresponding boundary conditions for Eqs.(1) and (2) are

$$u = w = 0, \quad \text{at } z = 0. \tag{5}$$

If the graphite lid is not bound to the susceptor, the boundary conditions on the top of the lid can also be assumed as

$$u = w = 0, \quad \text{at } r = 0 \quad \text{and } z = 0. \tag{6}$$

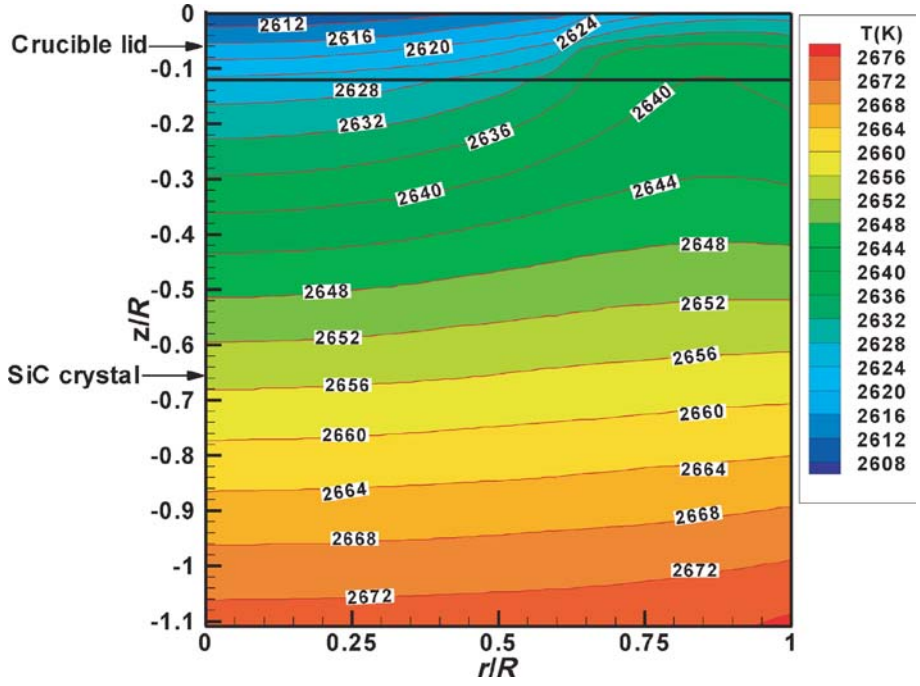

Fig. 3 Temperature distribution in the crucible lid and growing SiC crystal, $z/R = 0$–-0.1 for crucible lid, $z/R = -0.1$–-1.1 for silicon carbide

However, the stress distribution in the crystal will not change much by using boundary conditions (6) instead of boundary conditions (5). So we use boundary conditions (5) in our calculation of stresses.

At the central axis, the axisymmetric conditions are assumed,

$$u = 0, \quad \frac{\partial w}{\partial r} = 0, \quad \text{at } r = 0. \tag{7}$$

The growing interface and side surface of SiC crystal are considered as free of traction, that is,

$$\boldsymbol{\sigma} \cdot \boldsymbol{n} = 0, \quad \text{at } z = -H \quad \text{or } r = R, \tag{8}$$

where H and R are the height and radius of the crystal, respectively. At the crystal/lid interface, it is assumed that the two components are bound together during the growth, and no boundary conditions are set at the interface in the calculation.

As hexagonal crystals are isotropic in the basal (0 0 0 1) plane, $c_{11} = c_{22}$, $c_{13} = c_{23}$ in Eq.(3) and there are only five independent elastic constants. Since there are no experimental data with respect to elastic constants of SiC single crystal at high temperatures available, elastic constants at room temperature are used in our calculation, $c_{11} = 501 \pm 4$ GPa, $c_{33} = 553 \pm 4$ GPa, $c_{44} = 163 \pm 4$ GPa, $c_{12} = 111 \pm 5$ GPa, $c_{13} = 52 \pm 9$ GPa [11]. It is necessary to measure the elastic constants of SiC at high temperatures in future. As a first-order approximation, we assume that the elastic constants of SiC at high temperature are the same as those at room temperature. By extrapolating the experimental data of α of SiC in the temperature range of 200-1 500 K (see Fig. 2), the α-T relationship can be approximately expressed as

$$\alpha = A_1 \mathrm{e}^{-T/T_1} + A_2 \mathrm{e}^{-T/T_2} + A_3 \mathrm{e}^{-T/T_3} + \alpha_0, \tag{9}$$

where $A_1 = -5.54 \times 10^{-6}$, $T_1 = 3\,358.8$, $A_2 = -1.39 \times 10^{-4}$, $T_2 = 42.3$, $A_3 = -1.39 \times 10^{-4}$, $T_3 = 42.3$, $\alpha_0 = 8.83 \times 10^{-6}$. Accordingly, we can estimate that $\alpha_r = \alpha_\phi = \alpha_z \approx 6.3 \times 10^{-6}\,\mathrm{K}^{-1}$ at 2 600 K.

The following physical properties of graphite are taken from Ref. [13], $\alpha_r = \alpha_\phi = 0.95 \times 10^{-6} K^{-1}$, $\alpha_z = 28.09 \times 10^{-6} K^{-1}$ in the temperature range of 1 000 °C-1 800 °C, $c_{11} = 1\,060$ GPa, $c_{12} = 180$ GPa, $c_{13} = 15$ GPa, $c_{33} = 36.5$ GPa, $c_{44} = 4.5$ GPa at room temperature. We again assume that the elastic constants of graphite at high temperatures are the same as those at room temperature.

For the thermal stress calculation, a finite element scheme is developed in which eight-node quadrilateral elements are used for the discretization.

3 Results and discussions

For the calculation of electromagnetic field and temperature field in the growth system, we use an in-house built numerical code [4]. Figure 3 shows the temperature distribution in the composite structure of the growing SiC crystal and crucible lid. It can be seen that the axial temperature gradient in the crucible lid, which is on the top of the crystal, is greater than that in the SiC crystal. This is due to the fact that graphite has a lower thermal conductivity (about 29 W/(m·K)) than that of SiC single crystal (about 55 W/(m·K)) at temperature of 2 700 K. The positive temperature gradient in the radial direction ensures the expansion of the SiC crystal. The non-uniformity of the temperature field is the main cause of thermal stresses in the growing crystal.

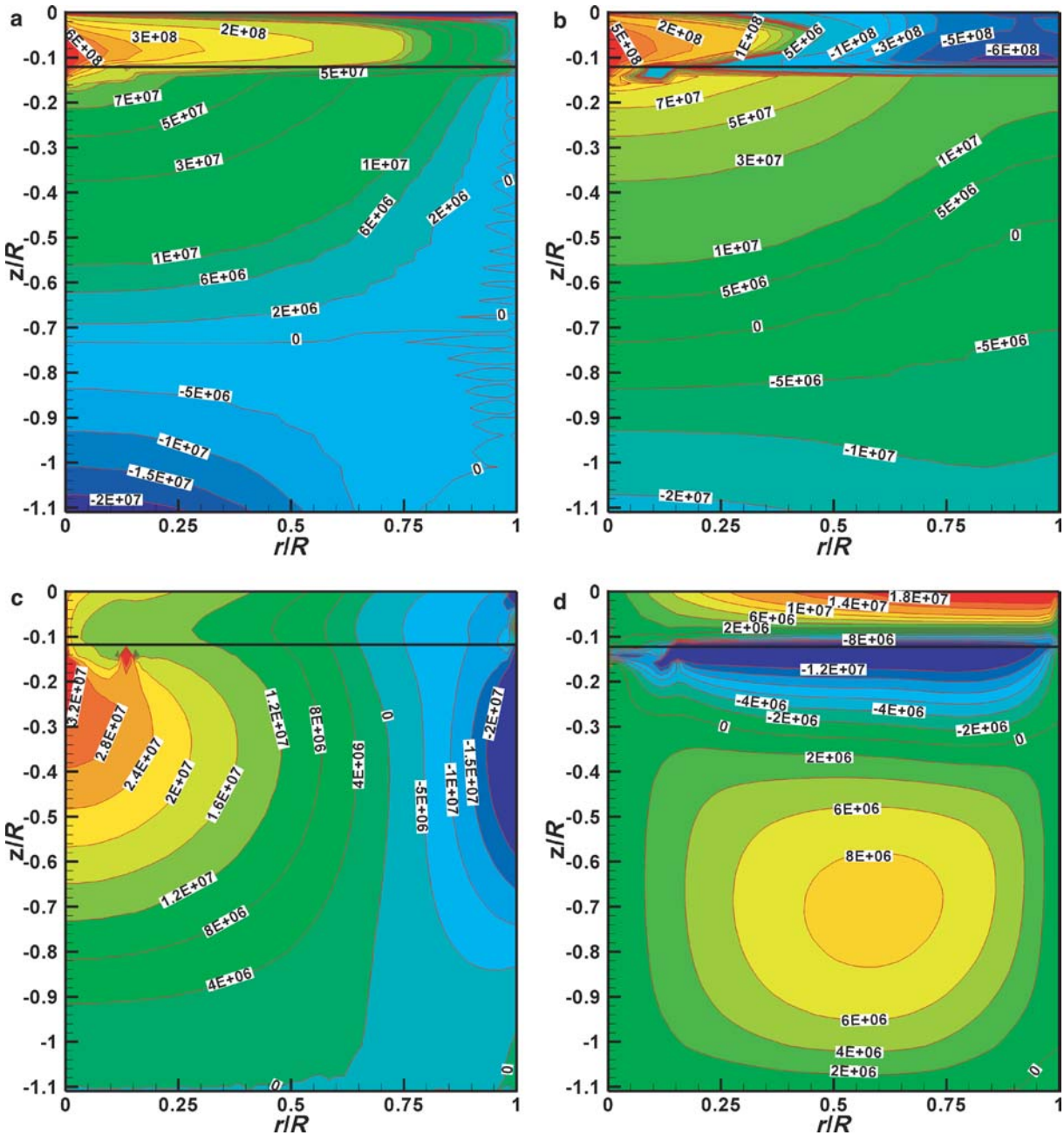

Fig. 4 Thermal stress distribution in the crucible lid and growing SiC crystal, $z/R = 0$--0.1 for crucible lid, $z/R = -0.1$--1.1 for silicon carbide. (a) σ_{rr}, (b)$\sigma_{\phi\phi}$, (c)σ_{zz}, (d) shear stress τ_{rz}

Figure 4(a) shows the distribution of stress component σ_{rr} in the composite structure of the SiC crystal and crucible lid. It can be seen that the maximum σ_{rr} in the crucible lid (about 1.4 GPa) is much higher than that in the SiC crystal (about 750 MPa). This is due to the difference of the product of thermal expansion coefficient α_r and elastic constant c_{11} between the crucible lid and SiC crystal. The thermal expansion coefficients α_r are about $0.95 \times 10^{-6}\,\mathrm{K}^{-1}$ and $6.3 \times 10^{-6}\,\mathrm{K}^{-1}$ for graphite and SiC crystal at 2 600 K, respectively, while the elastic constants at room temperature c_{11} are 501 GPa and 1 060 GPa, respectively.

Figure 4(b) gives the distribution of $\sigma_{\phi\phi}$, which shows a similar distribution pattern as σ_{rr}. They are both tensile stresses in the region near the seed and gradually change to compressive stresses toward the growth front. From Figs. 4(a) and 4(b) we can also see that the axial variations of these two stress components are larger than the radial ones. The maximum $\sigma_{\phi\phi}$ in the SiC crystal is about 600 MPa and occurs near the graphite lid.

Figure 4(c) shows that σ_{zz} is tensile in the region near the symmetry axis, and compressive in the region near the crystal periphery. It is shown that the maximum absolute values of

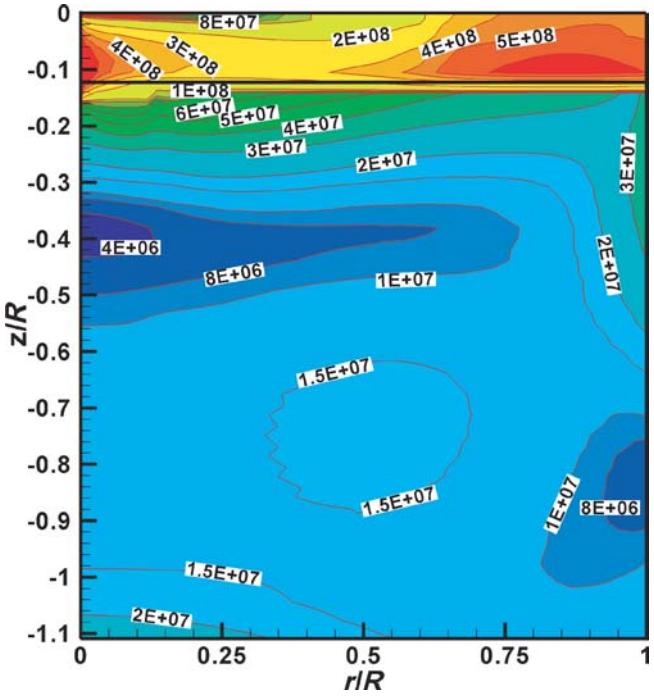

Fig. 5 The distribution of von Mises stress σ_{Mises} in the crucible lid and growing SiC crystal, $z/R = 0$ - –0.1 for crucible lid, $z/R = -0.1$ - –1.1 for silicon carbide

σ_{zz} are near the symmetry axis and at the crystal periphery. The radial variations of this stress component are much larger than the axial ones.

From Fig. 4(d) we can see that the sign of shear stress is positive in the graphite lid and changes to negative in the upper region of SiC, and then gradually changes to positive toward the middle region of SiC crystal. The maximum absolute value of shear stress in the crystal (about 20 MPa) occurs near the crucible lid. However, this value is much smaller than the maximum normal stress components σ_{rr} and $\sigma_{\phi\phi}$.

From Figs. 4(a)–4(d) we can see that both the distribution pattern and maximum stresses obtained by our new model are quite different from those given in Refs. [8, 9, 14]. In those references, the thermal expansion match between the SiC single crystal and graphite lid has not been considered in their thermal stress models. It is obvious that the thermal expansion mismatch between the crucible and SiC single crystal can significantly influence the distributions of thermal stresses in the growing SiC crystal.

According to the theory of Jordan et al. [8], it is assumed that dislocations are formed when the resolved shear stress, σ_{RS}, on a primary slip system exceeds the critical resolved shear stress, σ_{CRS}, and that dislocation density N is proportional to the difference between the resolved shear stress and the critical resolved shear stress on the slip plane, i. e. $N \propto (|\sigma_{RS}| - \sigma_{CRS})$. For 4H/6H SiC with hexagonal structure, gliding can occur in the basal (0 0 0 1) plane [14, 15], and the shear stress component, τ_{rz}, and the von Mises stress are usually used as the resolved shear stress [2–8]. Here the von Mises stress is defined by

$$\sigma_{\text{Mises}} = \sqrt{\frac{1}{2}[(\sigma_{zz} - \sigma_{rr})^2 + (\sigma_{zz} - \sigma_{\phi\phi})^2 + (\sigma_{\phi\phi} - \sigma_{rr})^2 + 6\tau_{rz}^2]}. \quad (10)$$

The distribution of von Mises stress is shown in Fig. 5. The axial variations of von Mises stress are higher than those in the radial directions. The maximum von Mises stress (about 600 MPa) in the crystal occurs in this region near the lid. While in the region near the axis and growth front, the magnitude of von Mises stress is relatively low. From Fig. 5 we can see that the maximum von Mises stress in the crystal significantly exceeds the critical resolved shear stress of less than 1 MPa at 2 200 °C-2 500 °C [5], so the plastic deformation and dislocation formation will take place in the crystal. The high von Mises stress in the region near the graphite lid will cause a relatively high dislocation density in the crystal near the graphite lid. However, it should be noted that the generation and multiplication of dislocations in the SiC crystal are non-linear functions of thermal stress and time [5]. The linear elastic model is only a qualitative description of thermal stresses.

4 Conclusion

Thermal stress distribution in the composite structure of the SiC single crystal and crucible lid is calculated using a finite element-based thermoelastic anisotropic model. The composite structure of the SiC crystal and crucible lid and thermal expansion match are considered in the thermal stress model for the first time. It is shown that the crucible lid has a great influence on the distribution of the thermal stress in the SiC crystal. Since the crucible lid and SiC crystal are bound together during the growth, the thermal stresses calculated by considering both the lid and crystal are more accurate than those obtained when only the crystal is considered. The predicted resolved shear stresses are much higher than the critical resolved shear stress of about 1 MPa. This implies that plastic deformation and dislocation formation will occur in the growing crystals. Our results show that in the region near the crucible lid, the crystal has a relative high dislocation density. However, it should be noted that the present linear elastic model is just a qualitative description of the thermal stresses. More studies on the plastic deformation and multiplication of dislocations in the growth of SiC crystals will be performed in future.

References

1. Chen, Q.S., Prasad, V., Zhang, H., Dudley, M.: Silicon carbide crystals — Part II: Process physics and modeling. In: K. Byrappa, T. Ohachi (eds.) Crystal Growth Technology, William Andrew/Springer-Verlag, 2003
2. Hofmann, D., Heinze, M., Winnacker, A., Durst, F., Kadinski, L., Kaufmann, P., Makarov, Y., Schäfer, M.: On the sublimation growth of SiC bulk crystals: development of a numerical process model. J. Cryst. Growth, **146**, 214–219 (1995)

3. Pons, M., Blanquet, E., J. Dedule, M., Garcon, I., Madar, R., Bernard C.: Thermodynamic heat transfer and mass transport modeling of the sublimation growth of silicon carbide crystals. J. Electrochem. Soc., **143** (11), 3727–3735 (1996)
4. Chen, Q.S., Zhang, H., Ma, R.H., Prasad, V., Balkas, C.M., Yushin, N.K.: Modeling of transport processes and kinetics of silicon carbide bulk growth. J. Cryst. Growth, **225**, 299–306 (2001)
5. Müller, St. G., Glass, R.C., Hobgood, H.M., Tsvetkov, V.F., Brady, M., Henshall, D., Jenny, J.R., Malta, D., Carter, C.H. Jr.: The status of SiC bulk growth from an industrial point of view. J. Cryst. Growth, **211**, 325–332 (2000)
6. Zhmakin, I.A., Kulik, A.V., Karpov, S.Yu., Demina, S.E., Ramm, M.S., Makarov, Yu. N.: Evolution of thermoelastic strain and dislocation density during sublimation growth of silicon carbide. Diamond and related materials, **9**, 446–451 (2000)
7. Selder, M., Kadinski, L., Durst, F., Hofmann, D.: Global modeling of the SiC sublimation growth process: prediction of thermoelastic stress and control of growth conditions. J. Cryst. Growth, **226**, 501–510 (2001)
8. Ma, R.H., Zhang, H., Ha, S., Skowronski, M.: Integrated process modeling and experimental validation of silicon carbide sublimation growth. J. Cryst. Growth, **252**, 523–537 (2003)
9. Ma, R.H., Zhang, H., Dudley, M., Prasad, V.: Thermal system design and dislocation reduction for growth of wide band gap crystals: application to SiC growth. J. Cryst. Growth, **258**, 318–330 (2003)
10. Lambropoulos John, C.: The isotropic assumption during the Czochralski growth of single semiconductors crystals. J. Cryst. Growth. **84**, 349–358 (1987)
11. Kamitani, K., Grimsditch, M., Nipko, J.C., Loong, C.K.: The elastic constants of silicon carbide: A Brillouin-scattering study of 4H and 6H SiC single crystals. J. App. Phys., **82**(6), 3152–3154 (1997)
12. Jordan, A.S., Caruso, R., von Neida, A.R., Nielsen, J.W.: A comparative study of thermal stress induced dislocation generation in pulled GaAs, InP, and Si crystals. J. App. Phys., **52**(5), 3331–3335 (1981)
13. Kelly B.T.: Physics of Graphite, Applied Science Publishers, 1981
14. Müller, G., Friedrich, J.: Challenges in modeling of bulk crystal growth. J. Cryst. Growth, **266**, 1–19 (2004)
15. Samant, A.V., Zhou, W.L., Pirouz, P.: Deformation of monocrystalline 6H-SiC. Mater. Sci. Forum. **264–268**, 627–630 (1998)